

# Coordinated Optimization of Generator Control System to Improve Transmission Capacity of Power System with Environment Friendly Effects

Guanhong Wang<sup>1\*</sup>, Taorong Gong<sup>1</sup>, Ying Li<sup>1</sup>, Yuting Liu<sup>1</sup>, Liming Jin<sup>2</sup>, Wenfeng Li<sup>1</sup>, Yong Tang<sup>1</sup>

<sup>1</sup> Department of Power System, China Electric Power Research Institute, Beijing 100192, CHINA

<sup>2</sup> Department of Power System, State Grid Chongqing Electric Power Company, Chongqing 400015, CHINA

\* Corresponding author: surpass99@126.com

## Abstract

Because the dynamic stability is limited by the large disturbance in power grid, and the system damping is insufficient after the N-1 fault, which leads to the reduction of transmission and transmission capacity. In order to improve the level of dynamic stability and the limited of generating capacity of the unit, the paper studies the coordinated optimization strategy of the generator excitation control system in disturbance. The results show that the excitation system and PSS have important influence on the dynamic characteristics of the power grid. Research shows that, the parameter configuration of the existing generators control system does not meet units full power generation requirements, which has not adapted to the development of power grid. At first, according to the strategy of optimization, we carried out on-site testing. The generator without compensation phase frequency characteristic hysteresis decreases about 10 degrees brought the compensation characteristics close to -90 degrees, in addition AC gain provided by PSS is increased about 50%. Then the phase compensation is carried out for the PSS parameters. The stability level in small disturbance and large disturbance has greatly improved. Research on Optimization and implementation strategy, ability can be safe, efficient, economy improving centralized power delivery.

**Keywords:** coordinated optimization, dynamic stability, excitation control, power deliveryability

Wang G, Gong T, Li Y, Liu Y, Jin L, Li W, Tang Y (2019) Coordinated Optimization of Generator Control System to Improve Transmission Capacity of Power System with Environment Friendly Effects. Ekoloji 28(107): 1123-1129.

## INTRODUCTION

The dynamic stability and frequency stability of the point to network after energy base outgoing system is connected to the power system is a key problem that restricts the transmission capacity of the power system (Guo et al. 2009, Mao et al. 2005, Xu 2011, Yang and Yang 2011, Zhao et al. 2009). AC/DC hybrid power system is complex in control, with many constraints on operation safety (Kundur 1994, Liu 2007, Shi et al. 2014, Wang and Guo 2006, Wang et al. 2008). Under the condition of ensuring the safe and stable operation of the unit, the parameters of generator excitation system, power system stabilizer and speed regulation system are optimized (Hu et al. 2017, Huang et al. 2011, Li et al. 2015, Liu et al. 1995, Mei et al. 2017, Xian and Li 2004, Zhu et al. 2004). Without increasing the more power system investment, it can improve the dynamic stability and outgoing capability of the energy base outbound system.

## STRUCTURE OF POWER SYSTEM

The access of large capacity units of a large energy base is concentrated through long lines. The A, B, C and D power plants at the sending end have 9 generating units connected to the HA substation. Among them, there are 25 600 MW units, and the load in HA area is about 450 MW, as shown in **Fig. 1**.

## STABILITY ANALYSIS

### Small Signal Disturbance Stability Analysis of the Power System

In the structure of power system shown in **Fig. 1**, the generator adopts self shunt excitation system, and the power system stabilizer is configured, and the speed governing system is a digital electro-hydraulic speed regulation system. The electric power of 10 units is sent over a long distance. Its dynamic stability level has great influence on the stability of the system. The calculation results of the latent root of small signal disturbance

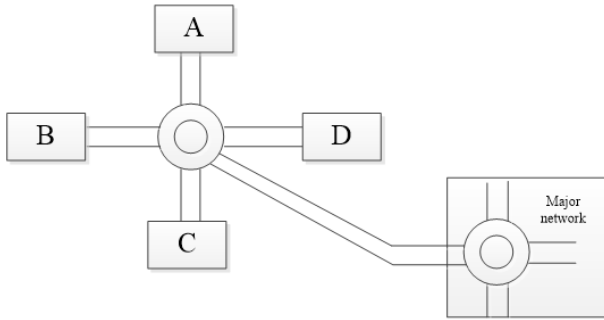


Fig. 1. Schematic diagram of Power System

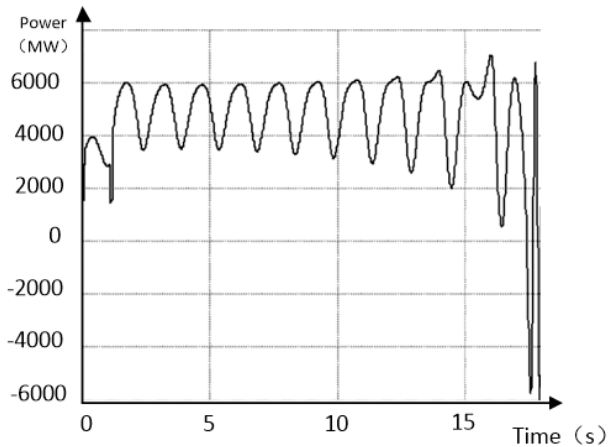


Fig. 2. Curve of active power oscillation with N-1 fault

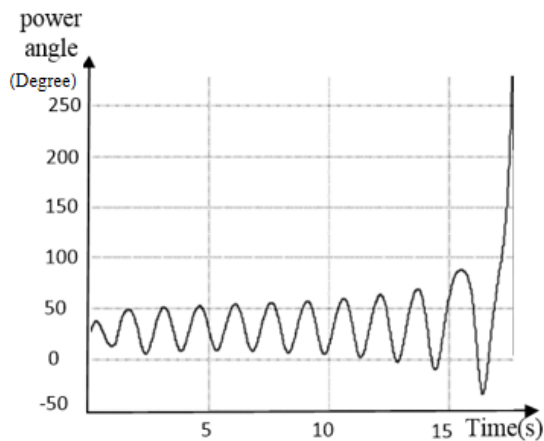


Fig. 3. The unit power angle oscillation with N-1 fault

show that there are 2 eigenvalues closely related to the sending terminal units. The first eigenvalue is  $-0.4996+j4.6555$ , the oscillation frequency is 0.74 Hz, and the attenuation damping ratio is 0.11. The second eigenvalue is  $0.3688+j5.3523$ , the oscillation frequency is 0.85 Hz, and the attenuation damping ratio is 0.06. Both of these 2 modes are strongly damped. The stable level of small signal disturbance is good.

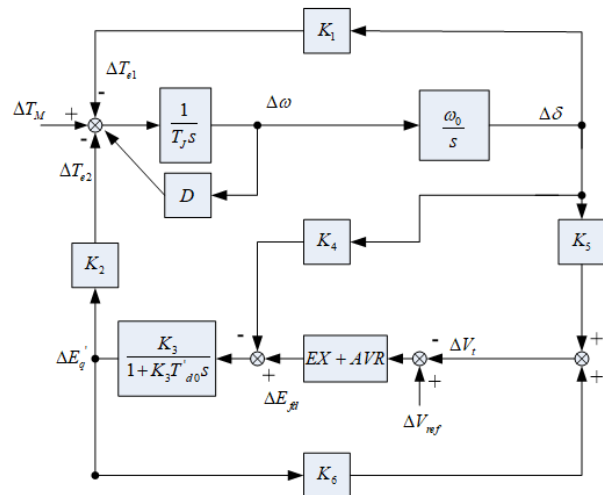


Fig. 4. Model of mechanism analysis

### Large Signal Disturbance Stability Analysis of the Power System

The unit of the sending end system is fully booting, and the external power of the transmission line is 5050 MW. When the N-1 disturbance occurs on the HA side of the HA-HB line, the dynamic instability will occur, and the oscillation frequency is 0.66 Hz. According to the requirement that the damping ratio of the power oscillation curve of the main transmission lines is not less than 0.015 after the large signal disturbance occurs, the large signal disturbance dynamic stability limit of the system is 4950 MW. Fig. 2 is a line power oscillation curve. Fig. 3 is the power angle swing curve of the terminal unit.

### INFLUENCE OF EXCITATION CONTROL ON DYNAMIC STABILITY AND PARAMETERS OPTIMIZATION

The Phillips-Heffron model usually takes account of the influence of speed control system and excitation system, and does not consider the coefficient of excitation system adjustment.

In Fig. 4, EX-AVR is the excitation system of the generator, and DGOV is the additional damping coefficient of the speed control system, which provides the mechanical torque of  $\Delta T_{M1}$ . The model is a single machine infinity model. By analyzing the effect of excitation system and additional control on K1-K6, the mechanism of adjusting the system parameters to affect the damping can be obtained.

Through calculation, it is concluded that the strong correlation coefficient with both operation condition and excitation system and PSS is Eqs. (1-2).

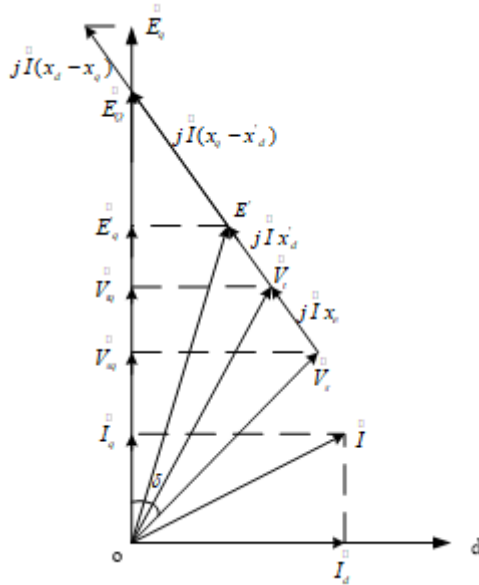


**Fig. 5.** Vector diagram of single machine infinite system

$$K_5 = \frac{v_{td0} V_s x_q \cos \delta_0}{v_{t0} x_{q\Sigma}} - \frac{v_{tq0} V_s x_d' \sin \delta_0}{v_{t0} x_d' \Sigma} \quad (1)$$

$$K_6 = \frac{v_{tq0} x_e}{v_{t0} x_d' \Sigma} \quad (2)$$

#### Adjustment Parameters Optimization of Additional Excitation

In the vector diagram of single machine infinite system shown in **Fig. 5**,  $x_e$  is the external reactance of the generator, the  $V_s$  is the infinite busbar voltage, the  $V_t$  is the generator terminal voltage, and  $\delta$  is the angle between the generator q axis and  $V_s$ , that is, the generator power angle. In addition, the imaginary potential after  $x_q$  reactance is  $E_Q$ , deducing the related quantities of reactive power and getting Eqs. (3-6):

$$i_d = (E'_q - V_s \cos \delta) / (x_d' + x_e) \quad (3)$$

$$i_q = \frac{V_s \sin \delta}{x_q + x_e} \quad (4)$$

$$v_{td} = x_q i_q = \frac{x_q V_s \sin \delta}{x_q + x_e} \quad (5)$$

$$\begin{aligned} v_{tq} &= E_Q - x_q i_d = E'_q - x_d' i_d \\ &= \frac{x_e}{x_d' + x_e} E'_q + \frac{x_d'}{x_d' + x_e} V_s \cos \delta \end{aligned} \quad (6)$$

The expression of the calculated reactive power is as follows

$$\begin{aligned} Q_e &= v_{tq} i_d - v_{td} i_q \\ &= \frac{1}{(x_d' \Sigma)^2} [x_e E_q'^2 + (x_d' - x_e) E_q' V_s \cos \delta - x_d' V_s^2 \cos^2 \delta] \\ &\quad - \frac{x_q}{(x_q \Sigma)^2} V_s^2 \sin^2 \delta \end{aligned} \quad (7)$$

The Eq. (7) is rewritten as the form of the deviation equation between  $\delta$  and  $E'_q$ , which is expressed as the following formula.

$$\begin{aligned} \Delta Q_e &= \frac{2x_e E_q' + (x_d' - x_e) V_s \cos \delta_0}{(x_d' \Sigma)^2} \Delta E_q' \\ &+ \left[ \frac{(x_e - x_d') E_q' V_s \sin \delta_0}{(x_d' \Sigma)^2} \right. \\ &\quad \left. + \frac{(x_q - x_d') (x_d' x_q - x_e^2)}{(x_d' \Sigma)^2 (x_q \Sigma)^2} V_s^2 \sin 2\delta_0 \right] \Delta \delta \end{aligned} \quad (8)$$

The generator's reactive power adjustment formula can be expressed as the following formula.

$$v_t' = v_t + X_c Q_e \quad (9)$$

In the type:  $X_c$  is the coefficient of adjustment.

Let  $V_X = X_c Q_e$ ,  $\Delta V_X$  is expressed as the deviation of  $\delta$  and  $E'_q$ , get Eq. (10).

$$\Delta V_X = K_9 \Delta \delta + K_{10} \Delta E_q' \quad (10)$$

In Eq. (10),

$$\begin{aligned} K_9 &= \left[ \frac{(x_e - x_d') E_q' V_s \sin \delta_0}{(x_d' \Sigma)^2} \right. \\ &\quad \left. + \frac{(x_q - x_d') (x_d' x_q - x_e^2)}{(x_d' \Sigma)^2 (x_q \Sigma)^2} V_s^2 \sin 2\delta_0 \right] X_c \end{aligned} \quad (11)$$

$$K_{10} = \frac{2x_e E_q' + (x_d' - x_e) V_s \cos \delta_0}{(x_d' \Sigma)^2} X_c \quad (12)$$

The calculation shows that the coefficients related to the adjustment coefficient are  $K_9$  and  $K_{10}$ , which are related to the running state of the system.

After considering the additional coefficient of adjustment, the Heffron model is optimized by the above analysis. Combined with the basic expression of the single machine infinite bus system in **Fig. 4**, we can get the deviation equations of  $\Delta T_e$ ,  $\Delta E'_q$ ,  $\Delta v_t$ ,  $\Delta \delta$  and so on are as follows.

$$\Delta T_e = K_1 \Delta \delta + K_2 \Delta E'_q \quad (13)$$

$$\Delta E'_q = \frac{K_3}{1 + T'_{do} K_3 S} \Delta E_{fd} - \frac{K_3 K_4}{1 + T'_{do} K_3 S} \Delta \delta \quad (14)$$

$$\Delta v_t = K_5 \Delta \delta + K_6 \Delta E'_q \quad (15)$$

$$\Delta \delta = \frac{\omega_0}{T_J S^2} (\Delta T_m - \Delta T_e) \quad (16)$$

$$\Delta V_X = K_9 \Delta \delta + K_{10} \Delta E'_q \quad (17)$$

The block diagram of Phillips-Heffron model with Reactive Current Compensation is made up of the above five formulas, as shown in **Fig. 6**.

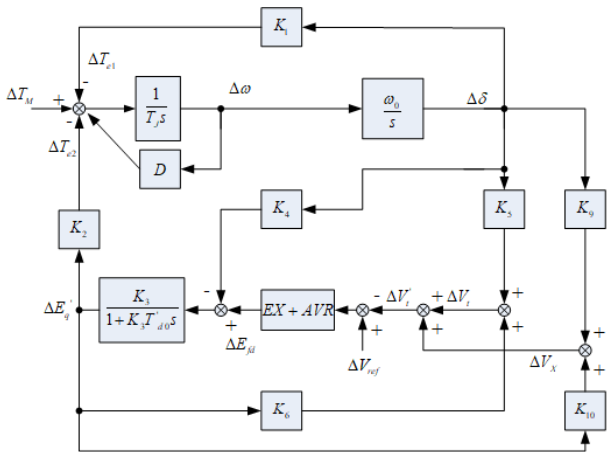


**Fig. 6.** Block diagram of Phillips-Heffron model with Reactive Current Compensation

The analysis shows that under different working conditions, the additional adjustment coefficient not only affects the increment of damping torque coefficient, but also affects the property of damping torque coefficient. The additional adjustment coefficient may produce a positive or negative damping torque coefficient increment. Similarly, negative additional adjustment coefficient may produce a positive or negative damping torque coefficient increment. The property such as positive or negative of the damping torque provided by additional adjustment is related to the load level of the unit. In the case of this paper, when the unit is loaded with large load, the damping torque coefficient provided by the negative additional adjustment is negative and the increment of damping torque coefficient provided by positive additional adjustment is positive.

**AVR Parameters Optimization in Excitation System**

Generator excitation control is the most important factor for the damping of the low-frequency oscillation of power system becoming weak or even negative damping (Huang and Han 2007, Huo et al. 2011, Tao et al. 2008, Wu and Zhu 2010, Zhang et al. 2015). In the model of **Fig. 6**,  $K_5$  and  $K_6$  are the parameters reflecting operation conditions, and  $K_6$  is always positive.  $K_5$  is positive when generator load is relatively small, but negative when load is large. This means that the damping of the low frequency oscillation mode is insufficient.

Before optimization, the transfer function of the main loop of the excitation system is Eq. (18). After optimization, the transfer function is Eq. (19).

$$G_1(s) = 500 \cdot \frac{1 + 1.0s}{1 + 10.0s} \cdot \frac{1}{1 + 0.01s} \quad (18)$$

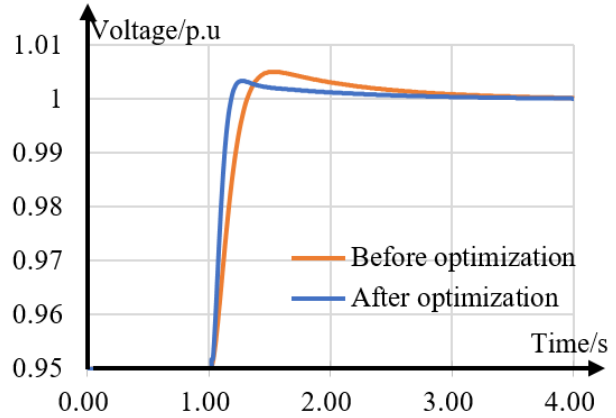


**Fig. 7.** The measured waveforms of the generator voltage response under step disturbance

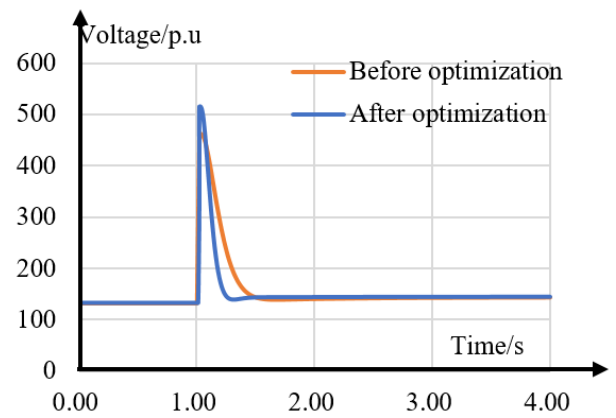


**Fig. 8.** The measured waveforms of the excitation voltage response under step disturbance

**Table 1.** Effect of excitation system main loop parameter optimization

parameter	rise time/s	peak time/s	overshoot /%
$G_1(s)$	0.16	0.86	7.0
$G_2(s)$	0.12	0.75	7.2

$$G_2(s) = 500 \cdot \frac{1 + 1s}{1 + 8.33s} \cdot \frac{1}{1 + 0.01s} \quad (19)$$

The above two sets of parameters are respectively used for testing under no load running state of generator. The step response characteristics of generator terminal voltage and excitation voltage are shown in **Figs. 7-8** and **Table 1**. The results show that to a certain extent, the optimization parameters reduce the system lag time which makes the voltage rise time shortened by 0.04s, and the adjustment time is shortened by 0.11s. It is beneficial to the dynamic response characteristics of the excitation system.

The uncompensated frequency characteristic of excitation system before and after AVR optimization is shown in **Fig. 9**. It can be seen that the generator phase lag decreases by  $10^\circ$  at the same frequency point. Based

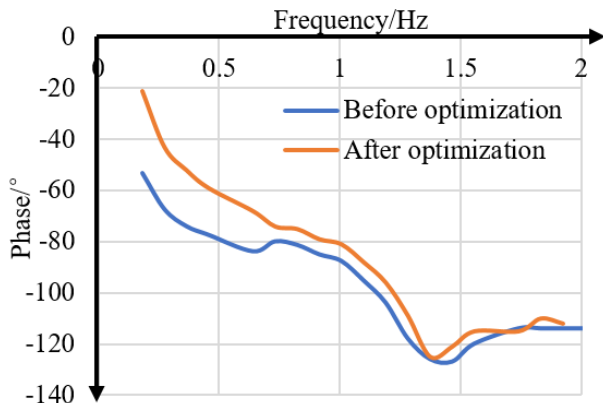


**Fig. 9.** The non compensated frequency characteristic before and after optimization

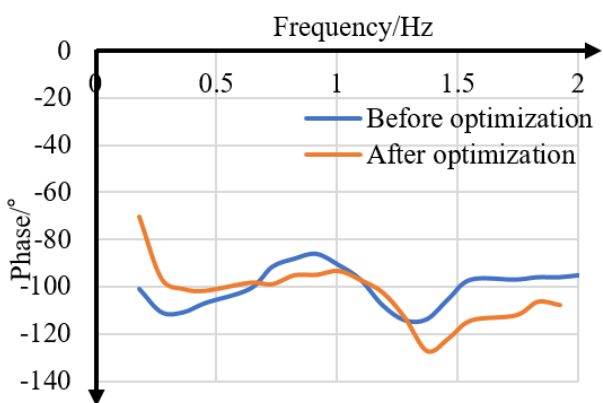


**Fig. 10.** The compensated frequency characteristic before and after optimization

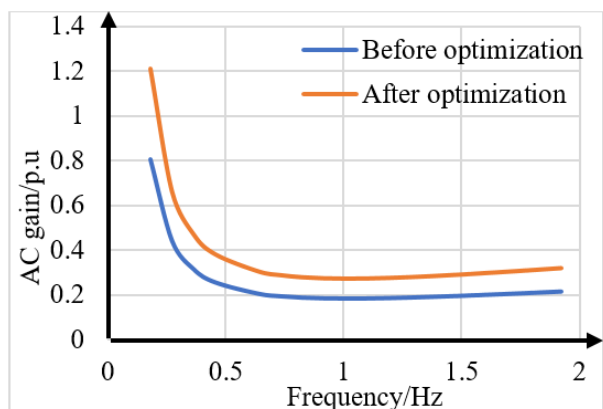


**Fig. 11.** The AC gain of PSS before and after optimization

on this, optimize the configuration of PSS. The compensation frequency characteristic of the generator after PSS is added is shown in **Fig. 10**. Compared with the previous optimization, the generator has better compensation frequency characteristics. In the concerned frequency range of 0.4-1.0 Hz, the compensation phase frequency characteristic of generator is basically close to  $-90^\circ$ . At the same time, the gain of PSS has also increased by nearly 50%. The gain

**Table 2.** Main parameters of PSS before and after optimization

Parameter name	Original parameter	Optimization parameters
$K_{S1}$	3	6
$K_{S2}$	0.67	0.67
$K_{S3}$	1	1
$T_1$	0.2	0.21
$T_2$	0.03	0.03
$T_3$	0.4	0.3
$T_4$	0.05	0.03
PSS Limiting valuc	0.05	0.1

before optimization is between 0.19-0.44. After optimization, the gain is increased to 0.28-0.67, as shown in **Fig. 11**.

### GENERATOR LOAD TEST CHECK

In this paper, the parameter optimization includes the time constant of the AVR main ring lag link, the PSS gain, the PSS first level, the second level advance, the lag time constant, the output limit and the additional adjustment coefficient. In order to fully verify the actual response of the unit before and after optimization, field tests were carried out. Taking A unit as an example, the operation parameters before and after optimization are shown in **Table 2**.

Under the condition of generator load, the load operation stability and the damping effect of optimized parameters after optimized parameters are tested. In the field test, the 2% step disturbance of generator terminal voltage is applied to excitation system. In the step test of PSS, the active power is oscillating 4.5 times. The first oscillation amplitude is 51 MW, as shown in **Fig. 12**. After PSS input, the active power is oscillating for 0.5 times. The first oscillation amplitude is 25 MW, as shown in **Fig. 12**. It can be seen that PSS has a good inhibitory effect on the local oscillation after input. During operation, the excitation voltage and excitation current of generator are stable without obvious fluctuation. Under the combined action of the optimized excitation system AVR and PSS, the unit can run normally and steadily, as shown in **Fig. 13**.

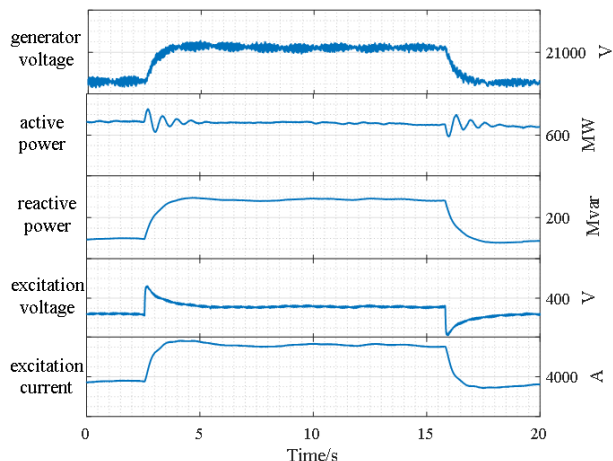


**Fig. 12.** Field test of generator voltage step without PSS in on-load

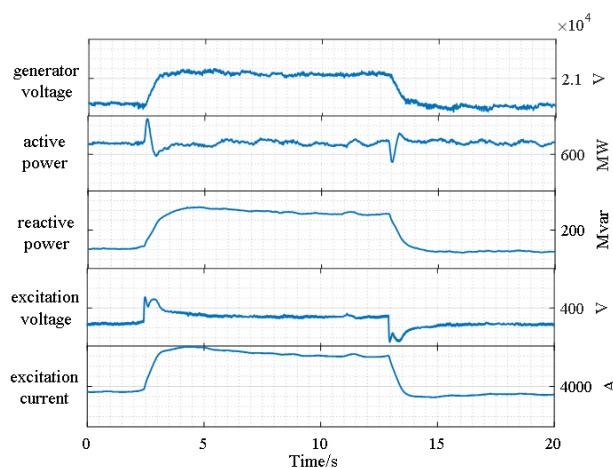


**Fig. 13.** Field test of generator voltage step with PSS in on-load

**EFFECT DETECTION AND CONCLUSION**

After the optimization of the control system and the field measurement, the dynamic response of the generator control system and the frequency response characteristic of the generator excitation system are greatly improved. The dynamic stability level and system stability of power system are enhanced.

The optimization of generator control system is based on simulation analysis, and then on-site implementation is carried out. After optimization, the delivery capacity of the system is greatly improved. Under the condition of maintaining the dynamic stability level of the same system, parameter optimization can add a new full-load 600 MW operation generating units and distributing electricity safely. The N-1 time domain disturbance comparison curve

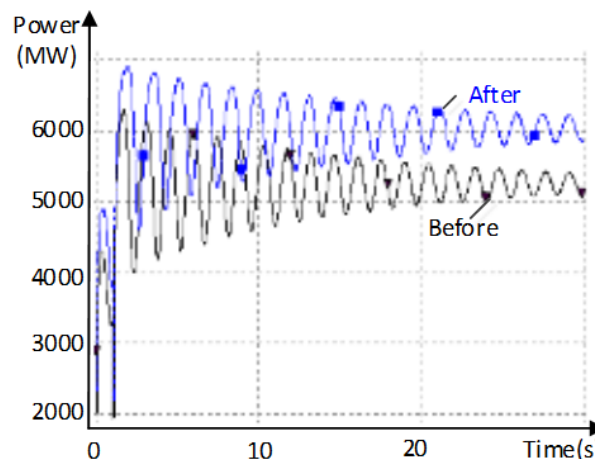


**Fig. 14.** Curves of the transmission capacity of HHV system before and after optimization (damping almost 0.015)

between 4750 MW sent by EHV before optimization and 5450 MW after optimization is shown in **Fig. 14**.

Generator excitation system, PSS and so on are important links that affect the dynamic stability level of the system. Comprehensive optimization of AVR parameters, additional adjustment, PSS amplification and lead lag time constant of excitation system can greatly improve system damping level. In this paper, the sending capacity of the system is constrained by the insufficient dynamic stability level. By configuring larger magnification and better phase compensation, the damping torque component used to study the excitation system of the power generation unit is greater, and then sufficient damping is obtained. The optimization technology of generator control system depends on simulation calculation, field test and measurement analysis. The change of parameters has a very important influence on the power production, and directly affects the safe and stable operation of the actual power system. Via optimizing research and implementation, we can improve the capacity of centralized power supply safely, efficiently and economically.

**ACKNOWLEDGEMENTS**

This work is supported by key project of smart grid technology and equipment of the National Key Research and Development Plan of China (2016YFB0900600), and Research on Improvement of Water Hammer Effect and Damping Lifting Method in High Proportion Hydropower System (SGCQ0000DKJS170086).

## REFERENCES

- Guo XJ, Bu GQ, Ma SY, Shen H (2009) System stability control strategy for multi-send & multi-infeed hvdc project from southwest hydropower stations to East China power grid. *Power System Technology* 2:52-58.
- Hu XF, Chen DZ, Zhang Y, et al. (2017) Impact of Multi-HVDC commutation failure on weak AC section and its countermeasures. *Electric Power* 50(05):26-32+51.
- Huang M, Han HY (2007) The PSS parameters optimization based-on power system operating variables. *Electric Power* (05):19-22.
- Huang Z, Zheng C, Pang XY, et al. (2011) Coordination control of DC active power for multi-circuit  $\pm 800$  kV DC power delivery system in Sichuan UHVAC/UHVDC hybrid power grid. *Power System Technology* 35(5):52-58.
- Huo CX, Liu ZH, Pu J (2011) Impact of reactive current compensation in excitation system on damping of power system oscillation modes. *Power System Technology* 35(5):67-70.
- Kundur P (1994) *Power system stability and control*. McGraw—Hill Inc, New York, 315-373.
- Li W, Chen T, Feng L, et al. (2015) Research on the difference mechanism and evaluation indices of ACDC control measures for improving frequency safety. *Electric Power* 48(11):54-59.
- Liu LJ, Wang MX, Li HJ, et al. (1995) Fast power control for the HVDC system in parallel with AC transmission. *Electric Power* (02):2-7+58.
- Liu Q (2007) *Power system stability and generator excitation control*. China Electric Power Press, Beijing, 388-413.
- Mao XM, Zhang Y, Guan L, Wu X (2005) Researches on coordinated control strategy for inter-area oscillations in AC/DC hybrid grid with multi-infeed HVDC. IEEE PES, Dalian, China.
- Mei Y, Zhou J, Lv YT, et al. (2017) Study on application of HVDC frequency limit control (FLC) in asynchronously interconnected Yunnan grid. *Electric Power* 50(10):64-70+77.
- Shi L, Luo Y, Zhu YH, et al. (2014) Real-time risk assessment method of small signal stability of power systems. *Electric Power* 47(05):39-43+52.
- Tao XY, Liu ZH, Zhao HG (2008) Study on the feasibility of wide usage of pss in multi-machine power system. *Power System Technology* 32(22):29-34.
- Wang GH, Tao XY, Li WF, et al. (2008) Influence of turbine governor on power system dynamic stability. *Proceedings of the CSEE* 28(34):80-86.
- Wang ZY, Guo ZZ (2006) Analysis on factors influencing transient stability limits of long-distance transmission profile. *Electric Power* (08):29-32.
- Wu KY, Zhu SZ (2010) Effect of reactive compensation for generator excitation system on PSS parameter setting and solution. *Electric Power Automation Equipment* 30(09):67-71.
- Xian YX, Li XY (2004) Optimal variable aim control strategy for improving transient stability of AC/DC systems. *Electric Power* (11):19-22.
- Xu PT (2011) Frequency control analysis for island system at seeding terminal in Yunnan-Guangdong UHVDC Transmission Project. *Electric Power Construction* 32(11):48-50.
- Yang D, Yang Y (2011) Real time simulation study on control system of Yunnan-Guangdong UHVDC transmission system in islanded mode. *Mechanical and Electric Engineering Technology* 40(10):70-74.
- Zhang JF, Li P, Li YS, et al. (2015) Risk analysis on optimization and setting for system reactive current compensation. *Automation of Electric Power Systems* 39(20):141-145.
- Zhao SS, Zhou ZG, Zhang DX, Yin YH (2009) Risk assessment index of dynamic stability for large-scale interconnected grids and its application. *Power System Technology* 33(2):68-72.
- Zhu F, Tang Y, Zhang DX, et al. (2004) Study on dynamic stability problems of AC interconnected area power grids in China and their solutions. *Power System Technology* 28(15):1-5.